Epitaxial films of GaInPAsSb quinary solid solutions

V. V. KUZNETSOV[1*], E. R. RUBTSOV[1], E. A. KOGNOVITSKAYA[2]

[1]St. Petersburg State Electrotechnical University, 197376, St. Petersburg, Prof. Popova 5, Russia

[2]Ioffe Physico-Technical Institute, 197376, St. Petersburg, Prof. Popova 5, Russia

The method of the obtaining quinary solid solutions on the basis of $A^{III}B^{V}$ compounds (GaInPAsSb) with specified properties was developed. New GaInPAsSb/GaSb, GaInPAsSb/InAs heterostructures were obtained to create optoelectronic devices for the 2–5 μm spectral range. The broken-gap type II hetero-junction was formed at the $InAs/Ga_{0.92}In_{0.08}P_{0.05}As_{0.08}Sb_{0.87}$ heterostructure, and a light-emitting diode was fabricated with the emission intensity maximum at 1.9 μm.

1. Introduction

The development of the fibre optical links of third generation based on the fluoride optical fibres with minimal dispersion and minimal optical losses requires operating on the middle infrared range (2–5 μm). Prospective materials for the optoelectronic circuit technology for this spectral range are narrow-band solid solutions based on $A^{III}B^{V}$ compounds (GaInPAsSb quinary solid solutions (QSS), in particular). Their advantage is the possibility of independent variation of three parameters: band gap, the lattice parameter and thermal expansion coefficient which become determinative when selecting the heteropair materials to form an ideal heterojunction.

The research was aimed to obtain quinary solid solutions on the basis of $A^{III}B^{V}$ compounds with specified properties and to obtain the new GaInPAsSb/GaSb, GaInPAsSb/InAs heterostructures for the fabrication of an optoelectronic device sensitive for the radiation in the 2–5 μm spectral range.

_____

*Corresponding author, e-mail: vvkuznetsov@mail.eltech.ru

2. Technology and research

The development of the heteroepitaxial technological process to obtain multicomponent solid solutions (MSS) from liquid phase was based on a comprehensive approach which can be divided into the following steps: providing conditions for the isoperiodic substitution; selection and justification of the thermodynamic model; determination of the miscibility gap for solid solutions with specified compositions within a specified temperature range; analysis of the liquid–solid interphase equilibrium; fabrication of the solid solution with the selected composition; analysis of the elastic strains at the heteroboundary; modelling of relaxation processes of interphase interaction at the heteroboundary. These steps are the basis for the development of multi-parametric technological process of the liquid phase heteroepitaxy of MSS of the specified properties.

Composition of the GaInPAsSb QSS was determined by the method of linear interpolation of the binary components using data from [1]. The band gap of the GaIn PAsSb QSS was interpolated as a combination of the band gaps of two quaternary systems (GaPAsSb and InPAsSb) with substitution of the metallic sublattice components and taking into account a non-linear contribution from the mixing effects [2]. Technological parameters of the liquid phase epitaxy (LPE) for fabrication the GaIn-PAsSb solid solution lattice-matched to InAs and GaSb were determined on the basis of the liquid–solid interphase equilibrium by a simple solution model [3–5]. The method of analysis and the main data for the calculation are given in [1, 2, 6–8]. Correction of the unreliable parameters of the interatomic interaction in the liquid phase between the elements P–As, P–Sb, As–Sb and the components of the solid phase GaP–GaSb and InP–InSb was carried out experimentally (the composition range of the solid phase was $Ga_{0.06}In_{0.94}P_{0.12}As_{0.8}Sb_{0.08}$ (InAs substrate) and $Ga_{0.05}In_{0.95}P_{0.10}As_{0.74}Sb_{0.16}$ (GaSb substrate)). The corrected interaction parameters allowed us to perform the reliable calculation of the liquidus and solidus compositions within the epitaxial process temperature range along the InAs and GaSb isoperiods on the both sides of the binodal space.

In the case of lattice mismatch between the layer and the substrate, elastic strains arise at the heteroboundary [2]. The coherent phase diagrams were used to take into account the contribution of the elastic strains into the liquid–solid heterophase equilibrium of the quinary systems. The equations for the coherent phase diagram of the $A^{III}B^{V}$-based $A_xB_{1-x}C_yD_zE_{1-y-z}$ quinary systems were derived using a simple solution model. The equations for the activity coefficients of the components in the elastically strained solid phase of the QSS were also obtained. The detailed derivation is given in [9]. The general equation of the coherent phase diagram of the quinary system has the following form:

$$\Delta S_{ij}^{F}\left(T_{ij}^{F}-T\right)+RT\ln\frac{4x_i^l x_j^l \gamma_i^l \gamma_j^l}{\gamma_i^{sl}\gamma_j^{sl}}=RT\ln x_i^s x_j^s + RT\ln \gamma_{ij}^{s,ex}+RT\ln \gamma_{ij}^{s,el} \qquad (1)$$

where ΔS_{ij}^F, T_{ij}^F are the entropy and the melting temperature of the components, respectively; γ_{ij}^s, γ_i^l, γ_j^l are the activity coefficients of the components in the liquid and solid phases; $x_{i,j}^l$ is the atomic fraction of the component in the melt.

To estimate the contribution from the elastic strains, the calculation of the contact supercooling ΔT_K was carried out using the interaction parameters from [2]. The calculation of the contact supercooling was carried out for the $Ga_xIn_{1-x}P_yAs_zSb_{1-y-z}$ quinary systems lattice matched to InAs and GaSb substrates at 773 K with lattice mismatch $f = -1\%$. It was shown that the negative values of the contact supercooling indicate the position of the thermodynamic instability boundaries of the QSS. Figure 1 shows the results of the calculations of the ΔT_K for the $Ga_xIn_{1-x}P_yAs_zSb_{1-y-z}$/InAs system at $T = 773$ K ($f = -1\%$, <111>).
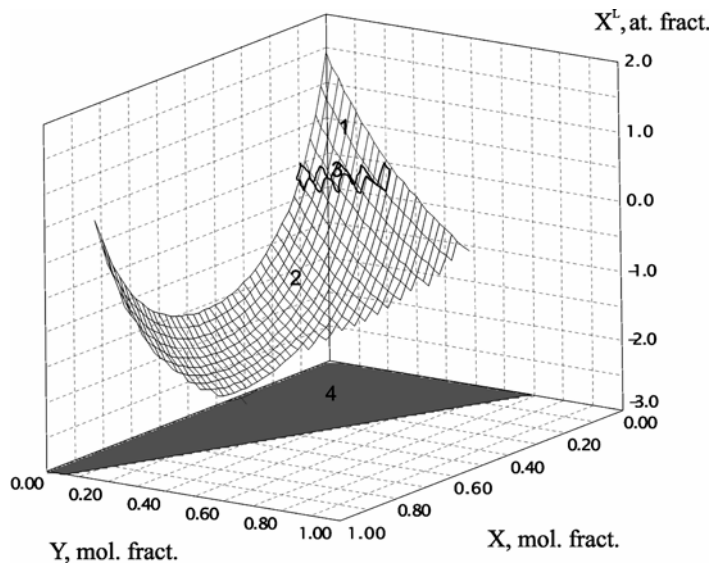
Fig. 1. Contact supercooling in $Ga_xIn_{1-x}P_yAs_zSb_{1-y-z}$/InAs system at 773 K, $f = -1\%$ ⟨111⟩: 1 – positive values, 2 – negative values, 3 – the range of circumzero values, 4 – a projection of the isoperiodic section

The analysis of the results shows that the areas of the negative contact supercooling, which coincide with the areas of the thermodynamic instability of the QSS, take a significant part of the phase space. It should be emphasized that this is connected with variation of the curvature of the dependence of the solid solution free energy on composition in these areas.

In the case of the layer–substrate lattice parameters mismatch, the elastic strains at the heteroboundary arise. This causes the stabilizing effect of the lattice parameter: the solid solution lattice parameter approaches that of the substrate. Elastic contribution to the total energy balance caused shift of the phase equilibrium and, hence, a modification of the solid solution composition. Quantitatively, this effect is de-

scribed by a stabilizing factor q [10, 11]. The equation to calculate the stabilization factor of the $A_xB_{1-x}C_yD_zE_{1-y-z}$ type quinary solid solutions was obtained in the following form:

$$q = 1 + 2\sigma[k_x^2(\delta_2\delta_3 - \beta_3^2) + k_y^2(\delta_1\delta_3 - \beta_2^2) + k_z^2(\delta_1\delta_2 - \beta_1^2) + 2k_xk_y(\beta_2\beta_3 - \delta_3\beta_1)$$

$$+\frac{2k_xk_z(\beta_1\beta_3 - \delta_2\beta_2) + 2k_yk_z(\beta_1\beta_2 - \delta_1\beta_3)]}{\delta_3(\delta_1\delta_2 - \beta_1^2) + \beta_3(\beta_1\beta_2 - \delta_1\beta_3) + \beta_2(\beta_1\beta_3 - \delta_2\beta_2)} \tag{2}$$

where $\sigma = V\lambda/a_s^2$, λ is the reduced modulus of elasticity, a_s is the substrate period, V is the molar volume, $k_x = \partial a/\partial x$, $k_y = \partial a/\partial y$, $k_z = \partial a/\partial z$, $\dfrac{\partial^2 G}{\partial y^2} = \delta_2$; $\dfrac{\partial^2 G}{\partial x^2} = \delta_1$;

$\dfrac{\partial^2 G}{\partial z^2} = \delta_3$; $\dfrac{\partial^2 G}{\partial x\partial y} = \beta_1$; $\dfrac{\partial^2 G}{\partial x\partial z} = \beta_2$; $\dfrac{\partial^2 G}{\partial y\partial z} = \beta_3$; where G is the free energy of one mol of QSS without elastic deformations.

The equation for the stabilization factor corresponds to the left-hand side part of the coherent spinodal equation [12] in which the denominator of the fraction corresponds to the chemical spinodal equation. This results in the stabilization factor approachings infinity at the boundary of the spinodal decomposition region. Therefore, the stabilizing influence of the substrate increases sharply near the composition areas confined by the chemical spinodal.

The calculation of the stabilization factor was carried out for the $Ga_xIn_{1-x}P_yAs_zSb_{1-y-z}$ solid solutions lattice-matched to GaSb and InAs at 773 K ($f = -1\%$). Figure 2 represents the results of the calculations of q for $Ga_xIn_{1-x}P_yAs_zSb_{1-y-z}$/InAs.
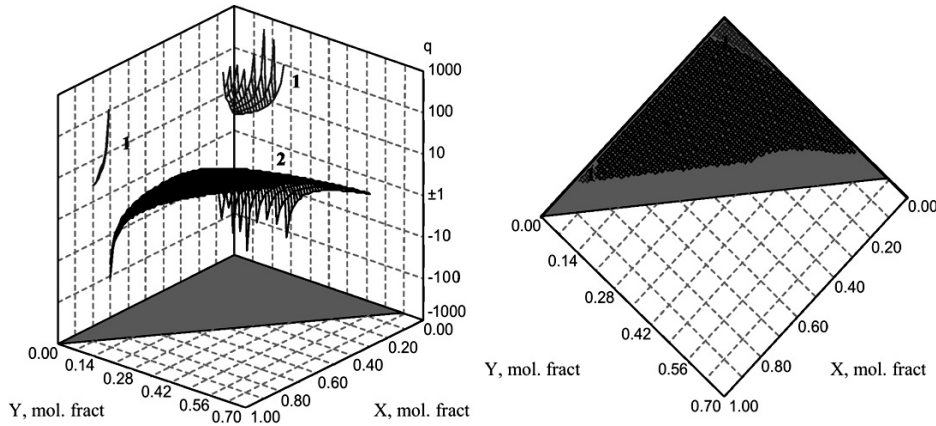

Fig. 2. Stabilization factor of $Ga_xIn_{1-x}P_yAs_zSb_{1-y-z}$/InAs system at 773 K, $f = -1\%$. $\langle 111\rangle$:
1 – positive values, 2 – negative values

Analysis of the results shows that within the area of the spinodal decomposition, the stabilization factor becomes negative. Similar to the case of the contact supercool-

ing, this happens due to the variation of the curvature of the dependence of the solid solution free energy on composition which leads to the change of the sign of Δa.

Fabrication of the semiconducting isomorphic QSS becomes more complicated due to the thermodynamic restrictions that arise not only because of the spinodal decomposition area, but also due to the fusibility restriction. The essence of the fusibility restriction is that at any temperature above the melting point of the most fusible component of the solid solution, a solid phase composition range exists for which the equilibrium liquid phase can not be found [13]. In the systems containing Sb this composition range shows itself at $T \sim 800$ K (since $T_{\mathrm{InSb}}^{F} = 798$ K). This restriction can arise also below the melting temperature of the most fusible component. This can be proven by the solidus isotherm that was calculated at $T = 793$ K for the AlGaInAsSb/GaSb system (Fig. 3). The analysis shows that the fusibility restriction arises reducing the amount of indium (as the solvent) and increasing the amount of antimony in the liquid phase up to ~ 0.5 atomic fraction (the amount of other component fracting is significantly smaller).
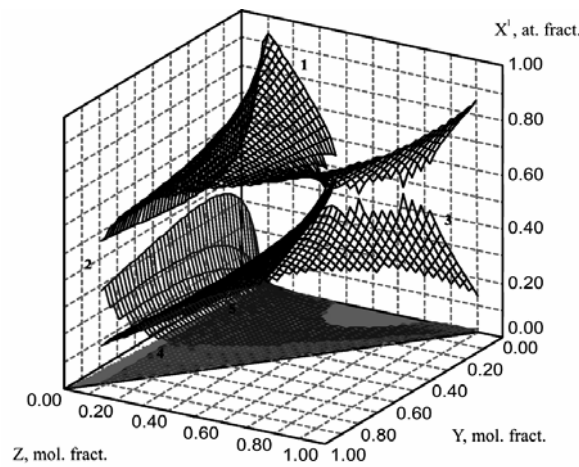

Fig. 3. Solidus isotherms of $Al_xGa_yIn_{1-x-y}As_zSb_{1-z}$/GaSb system at $T = 793$ K: 1 − In, 2 − Ga, 3 − Sb, 4 − As, 5 − Al

The calculation of the area of the fusibility restriction was carried out for the $Ga_xIn_{1-x}P_yAs_zSb_{1-y-z}$ system lattice-matched to GaSb and InAs. It was shown that the area of the fusibility restriction increases with temperature, while the thermodynamic instability area decreases. Therefore, the mutual effect of the fusibility restriction and thermodynamic instability leads to a decrease of the areas of the compositions of solid solutions that can be fabricated in these systems by LPE.

It should be noted that the elastic strains also influence the area of the fusibility restriction. This depends on the sign of the heteropair lattice mismatch (f). Analysis of the results of calculation of the liquidus isotherms (that was carried out for the $Ga_xIn_{1-x}P_yAs_z$ Sb_{1-y-z}/InAs system at 773 K shows that the area of the fusibility restriction decreases when $f < 0$, and increases when $f > 0$.

Based on the preliminary thermodynamic analysis, the interdependence between the thermodynamic parameters of the solid solution components, phase boundaries and the growth conditions of the GaInPAsSb QSS were obtained. In other words, the areas of restrictions should be taken into consideration for determination of the technological parameters of the heterostructure fabrication.

3. Experimental

LPE "step-cooling" method was used to grow the GaInPAsSb solid solutions on GaSb substrates from the Sb-rich melts in order to prevent the substrate subsolution and to reduce the concentration of the stoichiometric defects (V_{Ga} + Ga$_{Sb}$). GaSb (100) monocrystalline plates (n-type, Te-doped up to the concentration of $n = (1-5)\times10^{17}$ cm^{-3}) were used as the substrates. Epitaxial growth was preceded by homogenization of the melt at 923 K during 1–1.5 hour. The liquidus temperature (T^l) and the critical supercooling (ΔT_{cr}) were determined by the "in situ" method. Temperature range of the epitaxy process was 843–878 K, of the supercooling $\Delta T = 8$–17 K. The thicknesses of the obtained layers were 1–4 μm.

The GaInPAsSb QSS on the InAs substrates were grown from In-rich melts (to prevent the substrate subsolution process). Monocrystalline InAs <111> plates (400 μm thick) were used as the substrates. Homogenization of the melt was carried out at 993 K during 1.5 hour. The temperature range was 920–925 K, $\Delta T = 5$–9 K, the growth duration was 1–3 min, the thickness of the layers was 2–10 μm [14].

Compositions of the solid solutions were determined using the X-ray microanalyzer JXA–5 "Camebax", while the components distribution in the layer was measured by the secondary ion mass spectroscopy (SIMS) method. Estimation of the lattice parameters mismatch (LPM) between the layer and the substrate, and evaluation of the heterostructure crystal imperfection were done by the double crystal X-ray diffraction method. GaAs laser diode was used for the photoluminescence (PL) excitation and PL emission was recorded by a cooled ($T = 77$ K) InSb photodiode.

Solid solution was doped by Zn (acceptor) or Te (donor) to form the p-n heterojunction. Tellurium (in the composition of the Te-In hanging alloy) was placed into the melt just before the epitaxy process. Doping with Zn was done from the gas phase (by placing the In–Zn alloy into the specific temperature zone of the reactor). Zn concentration in the melt was determined by the vapour partial pressure of Zn, which was set by zone source temperature. Concentration of charged particles in the fabricated layers was 5×10^{17} cm^{-3}. Compositions of the fabricated Ga$_{1-x}$In$_x$P$_y$As$_z$Sb$_{1-y-z}$ epitaxial layers lattice-matched to GaSb were within the following ranges: $0.90 < x < 0.97$, $0.04 < y < 0.1$, $0.80 < z < 0.90$ [15]. Compositions of the grown Ga$_{1-x}$In$_x$P$_y$As$_z$Sb$_{1-y-z}$ epitaxial layers lattice-matched to InAs were within the ranges: $0.91 < x < 0.92$, $0.01 < y < 0.05$, $0.08 < z < 0.16$ and $0.07 < x < 0.1$, $0.07 < y < 0.13$, $0.77 < z < 0.81$. Table 1 shows the data for Ga$_x$In$_{1-x}$As$_y$P$_z$Sb$_{1-y-z}$/InAs solid solutions obtained from the experiment and from calculations.

Table 1. The experimental and calculations data for $Ga_xIn_{1-x}P_yAs_zSb_{1-y-z}$/InAs solid solutions

T, K	Composition of liquid phase (atomic fraction)				Composition of solid phase (mole fraction); 1 – calculation, 2 – experiment			
	$x_{Ga}^l \times 10$	$x_P^l \times 10$	$x_{As}^l \times 10$	$x_{Sb}^l \times 10$		x	y	z
925	0.0303	1.63	3.24	3.77	1	0.060	0.120	0.768
					2	0.08	0.08	0.81
					2	0.072	0.09	0.78
920	2.925	0.0862	0.24151	4.11	1	0.907	0.011	0.165
					2	0.92	0.012	0.165
					2	0.91	0.011	0.160

4. Results and discussion

Photoluminescence (PL) and electroluminescence (EL) methods were used to investigate the epitaxial layers. The investigations were carried out at 77 K (PL and EL) and 296 K (EL). 0.5×0.5 mm^2 chips with a point contact to the epitaxial layer and a uniform contact to the InAs substrate were used to measure EL.
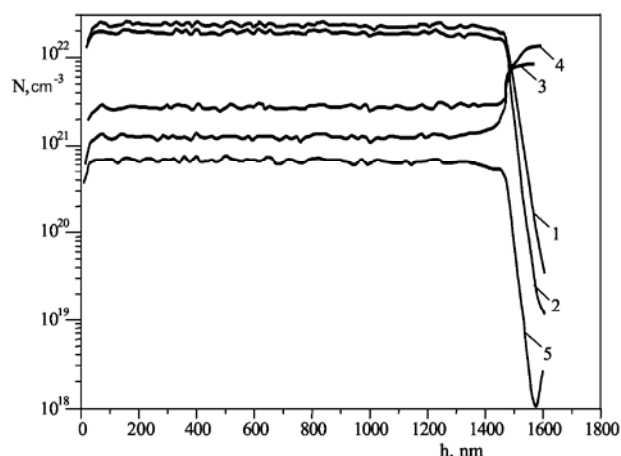

Fig. 4. Composition profiles of GaInPAsSb composition: 1 – In, 2 – As, 3 – Sb, 4 – Ga, 5 – P. h is the linear coordinate along the layer thickness

The structural perfection of the epitaxial layers of the $Ga_{1-x}In_xAs_yP_zSb_{1-y-z}$/GaSb solid solutions (SS) with compositions ranges: $0.90 < x < 0.97$, $0.80 < y < 0.90$, $0.04 < z < 0.1$ was evaluated from the results of the X-ray diffraction. Epitaxial layers had a mirror-like surface, lattice parameters mismatch was $1.5 \times 10^{-3} \leq f \leq 1.8 \times 10^{-3}$. Heterostructures had a good crystal perfection and for the best samples the X-ray rocking curves halfwidth was 30–40 arcsec. The existence of the abrupt heterojunc-

tions can be proven by the results of SIMS (Fig. 4). A sharp change of the concentra-
tion of components can be seen clearly on the layer–substrate boundary with the
boundary region width of about 50–70 nm). The PL wavelengths of the epitaxial lay-
ers were within 3.2–3.9 μm (T = 77 K), the radiation intensity of the QSS signifi-
cantly (3–7 times) exceeded the radiation intensity of the obtained quaternary
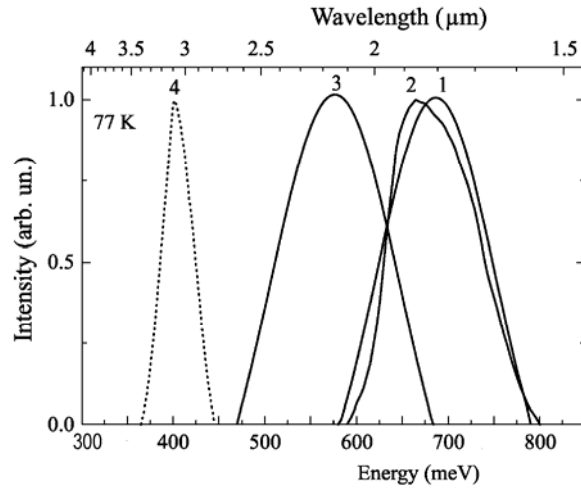GaInAsSb solid solutions [15] with the same band gaps.

Fig. 5. PL spectra of $Ga_{0.92}In_{0.08}P_{0.05}As_{0.08}Sb_{0.87}$/InAs heterostructure:
1 – undoped, 2 – Zn-doped, 3 – Te-doped, 4 – InAs substrate

The PL spectra of the $Ga_{0.92}In_{0.08}P_{0.05}As_{0.08}Sb_{0.87}$/InAs structure are shown in
Fig. 5. The maximum of the n-InAs substrate PL spectrum is at $h\nu$=400 meV, the
maximum of the SS PL spectrum is at $h\nu$ = 580–685 meV. PL maximum of the pur-
posely undoped GaInPAsSb solid solution ($h\nu$ = 690 meV) is conditioned by the tran-
sitions between the conduction band and the double-ionized acceptor levels. This
explains a significant FWHM of the PL spectrum ($\Delta h\nu$ = 100 meV). Doping the solid
solution with Zn (as an acceptor) leads to the recombination to the deeper acceptor
level and produces a spectrum shift (~20 meV) to the lower energies with the same
spectrum halfwidth. Doping with donor (Te) leads to the compensation of the p-type
conductivity, hence the SS layers demonstrate a slight n-type conductivity. The PL
maximum of the Te-doped SS shifts by 110 meV to lower energies ($h\nu$ = 580 meV) in
comparison to undoped SS. The band gap of the $Ga_{0.92}In_{0.08}P_{0.05}As_{0.08}Sb_{0.87}$ SS meas-
ured at 77 K is 695 meV [14].

Studies of EL of the InAs/GaInPAsSb heterostructures were carried out. The in-
terpretation of the experimental results was done in the framework of the broken gap
type II heterostructure luminescence model [16].

Both the substrate–layer heterostructures and the homo p–n junction structures in
the bulk n-InAs/P-GaInPAsSb/N-GaInPAsSb SS were used for the EL investigation.

The current–voltage characteristics of the p-P, p-N, n-N and n-P structures changed insignificantly within the 77–300 K temperature range, indicating the tunnelling current flow. The isotype p-P and N-n structures demonstrated rectifying characteristics and produced EL in the 77–300 K temperature range, whereas the P-n structure showed no rectification nor EL. This fact confirms that in the grown InAs/GaInPAsSb structure the type II heterojunction was formed.

Analysis of the EL spectra (Fig. 6) of the n-N-p (at 77 K) and n-P-N (at 77 and 300 K) structures showed that in the both cases the spectra consist of two bands: the short-wave band (685–695 meV, 77 K), produced by the recombination emission in the SS, and the long-wave band (400 meV, 77 K) due to the recombination emission in the substrate. At 300 K the emission maxima are at 640 and 360 meV.
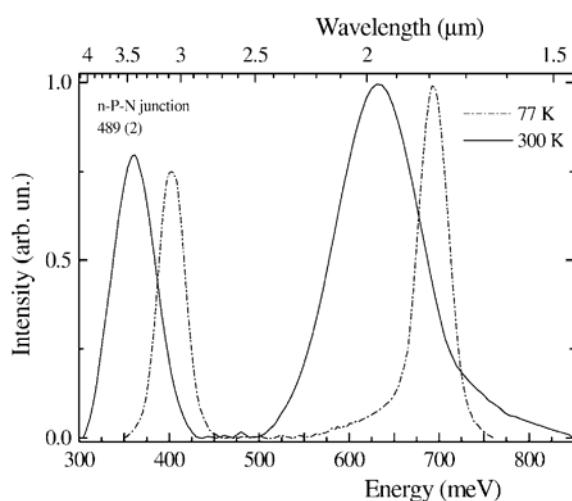

Fig. 6. EL spectra of the n-InAs/P-GaInPAsSb/N-GaInPAsSb structure

The temperature shift of the maxima correspond to the temperature dependence of the InAs band gap (3×10^{-4} eV/K) which speaks for a good crystal perfection of the epitaxial layer. It is assumed that in the homo-p-n heterojunction of the SS, similarly as in InAs, the p-region becomes the emitting region, since the electron diffusion length exceeds that of holes. This is supported by the close matching of the PL spectra of the p-type material of the SS and the EL spectra of the P-N junction.

On the basis of the homo-p-n junction in the bulk SS the LEDs were fabricated with the radiation maximum at 1.9 μm and FWHM of the spectrum amounting to 0.3 μm.

5. Conclusion

A comprehensive thermodynamic analysis of the quinary Ga–In–P–As–Sb system was carried out. The epitaxial layers of the $Ga_xIn_{1-x}P_yAs_zSb_{1-y-z}$ QSS on the (100)

GaSb substrates within the composition range $0.9 \leq x \leq 0.97$, $0.04 \leq y \leq 0.1$, $0.80 < z < 0.90$ and on the (111) InAs substrates ($0.91 < x < 0.92$, $0.08 < y < 0.16$, $0.01 < z < 0.05$) were formed. It was shown that in the $Ga_{0.92}In_{0.08}P_{0.05}As_{0.08}Sb_{0.87}$/InAs heterostructure, the broken gap type II heterojunction is formed which became a basis for the development of the light-emitting diode and photodiode with the emission intensity and photosensitivity maximum at the 1.9 μm range.

Acknowledgement

References

[1] RUBTSOV E.R., SOROKIN V.S., KUZNETSOV V.V., Russian J. Phys. Chem., 71 (1997), 415.

[2] KUZNETSOV V.V., MOSKVIN P.P., SOROKIN V.S., *Nonequilibrium Effects in Liquid-Phase Heteroepitaxy of Semiconductor Solid Solutions*, Moscow, Metallurgiya, 1991 (in Russian).

[3] GUGGENHEIM E.A., *Thermodynamics*, 3rd Ed., North-Holland, Amsterdam, 1957.

[4] GIL'DENBRANT G., *Nonelectrolytes Solubility*, Moscow, 1938.

[5] OLCHOWIK J.M., Phys. Stat. Sol. A, 142 (1994), 415.

[6] OLCHOWIK J.M., Phys. Stat. Sol. A, 146 (1994), K19.

[7] RUBTSOV E.R., KUZNETSOV V.V., LEBEDEV O.A., Inorg. Mater., 34 (1998), 525.

[8] KUZNETSOV V.V., STUS N.M., TALALAKIN G.N., RUBTSOV E.R., Crystall. Rep., 37 (1992), 998.

[9] KUZNETSOV V.V., RUBTSOV E.R., RATUSHNYI V.I., KOGNOVITSKAYA E.A., Crystall. Rep., 49 (2004), 193.

[10] OLCHOWIK J.M., SADOWSKI W., SZYMCZUK D., J. Cryst. Growth, 158 (1996), 241.

[11] SOROKIN V.S., Crystall. Rep., 31 (1986), 844.

[12] KUZNETSOV V.V., RUBTSOV E.R., Russian Tsvetn. Metallurgiya, 3 (1997), 57.

[13] OLCHOWIK, J.M. SADOWSKI W., SZYMCZUK D., J. Cryst. Growth, 153 (1995), 11.

[14] AIDARALIEV M., ZOTOVA N.V., KARANDASHOV S.A., MATVEEV B.A., REMENNYI M.A., STUS N.M., TALALAKIN G.N., SHUSTOV V.V., KUZNETSOV V.V., KOGNOVITSKAYA E.A., Semiconductors, 36 (2002), 944.

[15] KUCHINSKII V.I., VASIL'EV V.I., GAGIS G.S., DERYAGIN A.G., DUDELEV V.V., Proc. of LFNM 2003, 5th International Workshop on Laser and Fibre-Optical Networks Modelling, Kharkov (Ukraine) 19–20 Sept. 2003, p. 76.

[16] MIKHAILOVA M.P., TITKOV A.N., Semicond. Sci. Technol., 9 (1994), 1279.